

# Experiences and Practical Hints on Using the DDRP Method, Illustrated by the Example of the $H_2 + H$ Reaction

Gy. Dömötör,<sup>1</sup> M.I. Bán,<sup>1\*</sup> and L.L. Stachó<sup>2</sup>

<sup>1</sup>Institute of Physical Chemistry, Attila József University, P.O. Box 105, H-6701 Szeged, Hungary, and <sup>2</sup>Bolyai Institute for Mathematics, Attila József University, Aradi Vértanúk tere 1, H-6720 Szeged, Hungary

Received 7 April 1993; accepted 2 July 1993

By using the dynamically defined reaction path (DDRP) method and starting from various initial polygons, the intrinsic reaction coordinate (IRC) of the  $H_2 + H \rightarrow H + H_2$  reaction has been calculated. The numerical stability of the method is illustrated by the evolution phases of the reaction path. Techniques and experiences on the parameter choice and effects of the parameter values on the stability and computer time consumption are discussed. © 1993 by John Wiley & Sons, Inc.

## INTRODUCTION

For searching intrinsic reaction coordinates (IRCs) and locating critical points (CPs) on potential energy surfaces (PESs) of chemical reactions, a new curve variational [so-called dynamically defined reaction path (DDRP)] method<sup>1-3</sup> was recently suggested. The pure theoretical foundation of the procedure<sup>2</sup> requires an analytic coercive function with Morse-type CPs. The first numerical illustrations<sup>1,3</sup> were applied to polynomial functions satisfying this criterion. However, the energy functions of atomic configurations are noncoercive and, to our knowledge, almost nothing is known about their analytic properties and precise behaviors up to the second order around the CPs. It can, nevertheless, be expected that the PESs can be approximated uniformly (up to any order) by analytic functions having finitely many CPs of Morse types located arbitrarily close to the real CPs. In this case, the coercivity plays merely a technical role. Such a function can be modified by adding to it an auxiliary function having small values and derivatives on some given domain containing the CPs and tending rapidly to infinity outside this domain. By structural stability,<sup>4</sup> steepest descent paths (SDPs) and CPs can be approximated uniformly in this manner. It readily follows that this adjustment can well be simulated by a numerically much simpler method, namely, given a region with piecewise smooth boundary (e.g., a multidimensional ball or a rectangular polytope) containing the CPs, we may project the overflowing pieces of the trial curves to the boundary in each step. In chemical practice, where we always know not too large a

*priori* regions outside of which the energy function changes irrelevantly little, the problem of coercivity is settled satisfactorily. On the other hand, it can be expected that the condition of analyticity in the theoretical work<sup>2</sup> can drastically be weakened. (The proofs may, of course, become essentially even more complicated.) Therefore, we can hope that any of the frequently applied quantum chemical (semiempirical or *ab initio*) methods coupled with our procedure can be used without further adjustments if we require polygon approximations of the IRCs with not too small edges. Due to the iterations involved, such methods for approximating the energy function provide functions that are piecewise analytic. However, we have no practical information about boundaries of such domains of analyticity and we cannot expect a continuous coincidence of the calculated values of two neighboring domains. If the discontinuities are small with respect to the edges of the IRC-approximating polygons, satisfactory results can still be expected. One of the main purposes of this article is to show on perhaps the simplest practical case of the collinear  $H_2 + H \rightarrow H + H_2$  reaction that the DDRP procedure,<sup>5,6</sup> works in a stable way even with a theoretically badly behaving semiempirical energy function. In a next article,<sup>7</sup> we are going to apply the same technique<sup>5,6</sup> to obtain IRCs of various collinear reactions of three atoms (H atoms and halogens) not yet investigated from this point of view. Searching for IRCs of reactions with configuration spaces of higher dimensions requires effective parallelization. From the experiences gained when working on this subject,<sup>8</sup> we may conclude that 100-times vectorization can make reactions practically treatable up to 10 atoms. Of course, it is not yet foreseeable whether some adjustment of the numerical procedure for calculating the energy function will or will not be necessary in such complicated cases.

## DISCUSSION

Almost all known methods<sup>9-11</sup> work principally in the same way, searching for the reaction path (RP) either by walking SDPs in a "gutter" (or "bobsled track") from one into another valley through the col or by finding first the saddle point (SP) and then descending from it into the valleys/minima, again by SDPs. Such methods proved to be satisfactory for conventional computers and searching procedures because they are rapid enough and in most cases assure convergence. Nevertheless, their disadvantages are that they tend to be unstable when following curved and bifurcating paths and they are parallelizable only in the program segments of computing single gradient values of the energy function. Therefore, they cannot be run effectively on the most modern vector computers. An obvious alternative to such up/downhill methods is searching for RPs "crosswise" (transversely) in the gutter. A drop of rain or a ball on the wall of the eaves trough will always find their way into the draining well or sink hole and their motion will be controlled by the slopes of the walls and the bottom of the gutter. In exactly the same way, the virtual motion of a point selected on a PES will be guided by the actual vector field generated by, e.g., a quantum chemical method. Mathematical algorithms can therefore be constructed to follow the motion of the selected point directed by the actual vector field on its trajectory through the PES. The philosophy of our method therefore is this: Let us first choose a polygon† in the multidimensional configurational space of the problem to be investigated. Now, set out points uniformly distributed on the edges of the polygon ("stringing of pearls") and use a (semiempirical or *ab initio*) quantum chemical method to calculate the energy of the actual chemical system and the gradients or some approximating values of them at the chosen points. Move the points with determined steplengths toward the directions of the negative gradients. By the effect of the vector field, the original uniform distribution of the points ("a string of pearls") will be changed: In the directions of the minima (attractor regions), the points begin crowding while in the neighborhood of the SP they are going to become sparser. This will finally result in the separation at the middle of the approximating curve into two pieces (the string of pearls splits and the beads will run down the two far ends of the strings). Therefore, it is practical to use a homoge-

nizing procedure after several calculational steps assure permanently the uniform distribution of points.

One of the most important features of our D algorithm<sup>5,6</sup> is its high numerical stability, which is not influenced even by the differential topology complexity (e.g., the existence of several multistationary states) of the PES that has been illustrated by a convincing example.<sup>3</sup> By using an artificial mathematical function,<sup>1</sup> this example has shown when starting even from an almost hopeless position of an initial curve that crossed itself several times we can safely reach the final IRC passing through all the stationary points (four minima and three saddle points) of the PES. Because the fundamental of our method is to find RPs and their extrapoints on PESs, in the present article we would like to illustrate further the procedure and show its nature on a simple and well-known chemical reaction before using it routinely to calculate various less complicated chemical systems.<sup>7,15</sup> For the sake of simplicity and rapidity, we chose the  $H_2$  reaction and the MNDO quantum chemical approximation.\*

Three parameters controlling the convergence of the iterations seem to be particularly important: parameter  $\eta$  controls the lengths of steps taken defining the points  $P'_1, P'_2, \dots, P'_n$  of the next approximating polygon from the points  $P_i$  of the former one by

$$P'_i = P_i + \eta \nabla U(P_i)$$

Here,  $U$  stands for the potential energy and  $\nabla U$  is gradient operation. Our experiences show that big steplengths may jeopardize convergence. Therefore, a parameter  $\sigma$  is used to prevent taking too large steps in formula (1). If

$$\eta \|\nabla U(P_i)\| > \sigma$$

holds for some point  $P_i$  then instead of one big step several smaller steps of type (1), with  $\eta_j$  instead of  $\eta$ , satisfying

$$\eta_j \|\nabla U(P_i)\| < \sigma$$

will be performed. (As usual, we identify points by their position vectors and write  $\|\cdot\|$  for Euclidean length.) The resulting new vertices  $P'_1, \dots, P'_n$  tend to accumulate around the stationary points of the PES. To get a faithful representation of the continuous curve by the constructed successive polygons, a homogenization procedure determined by edge length parameter  $\epsilon$  has to be applied to  $P'_i$ . In the course of this procedure, the distance  $\|P'_i - P'_{i+1}\|$  of each neighboring pair of vertices consecutively checked. If  $\|P'_i - P'_{i+1}\| \geq \epsilon$ , the

\*Lotard's ("chain-") method<sup>12-14</sup> is such a method; it contains the seeds of a method similar to ours. However, it tries to generate the points of the next approximating polygon in a presumably orthogonal direction of the represented ideal approximating curve. Because the ideal curve cannot be restored by simple interpolations from a finite family of its points, the resulting polygons by such a method may essentially be different from the desired ones even if small steps are used.

†The DDRP procedure is, of course, independent of the character of the quantum chemical method used for computing energy function.

\* Author to whom all correspondence should be addressed.  
† Siegel type, in the terminology of refs 1 and 2.

(accidentally multidimensional) edge  $P'_i, P'_{i+1}$  will be divided into  $n_i = \lceil \|P'_i - P'_{i+1}\|/\epsilon \rceil$  equal parts, resulting in the points

$$P''_{j(i)} = P'_i, P''_{j(i)+1}, \dots, P''_{j(i)+n_i} = P'_{i+1} \\ j(i+1) = j(i) + n_i \quad (4)$$

of a new approximating polygon. To avoid too large numbers of points, if  $\|P'_i - P'_{i+1}\| < \epsilon$  then the vertices  $P'_{i+1}, P'_{i+2}, \dots$  will be omitted until we get a value  $> \epsilon$  for the sum of their consecutive distances. Hence, we get the new points

$$P''_{j(i)} = P'_i, P''_{j(i)+1} = P'_{k(i)}; \\ \sum_{i=1}^{k(i)-1} \|P'_i - P'_{i+1}\| \leq \epsilon < \sum_{i=1}^{k(i)} \|P'_i - P'_{i+1}\| \quad (5)$$

Thus, by (4) and (5) we obtain the polygon  $P''_i = P''_1, P''_2, \dots, P''_{k(n)} = P'_n$  satisfying

$$\|P''_i - P''_{i+1}\| < \sup_{\delta \leq \epsilon} \delta / [\delta / \epsilon] = 2\epsilon \quad (6)$$

which can be used as initial data for a further step. These steps are continued one after the other until achieving convergence. The criteria of convergence are discussed in ref. 2 and can be formulated in terms of the Hausdorff distance<sup>5,6</sup> between two consecutive approximating polygons.

If we start from a closed polygon, the convergence of the procedure can easily be verified. In this case, the area of the polygon tends to become zero, i.e., the edges of the polygon represented in a plane shrink to a 1-D line.\*

To justify the stability of the algorithm, we started from different initial curves constructed of various polygons. The computations were carried out on an IBM-compatible AT 286 PC equipped by an arithmetical coprocessor 80287 and were designed to supply comparable results by using a fixed set of the parameters  $\epsilon, \eta,$  and  $\sigma$ . The parameters were kept fixed at values  $\epsilon = 0.3, \eta = 0.002,$  and  $\sigma = 0.003$  during the whole procedure although the algorithm would have permitted immediate alterations. The choice of parameters was motivated by results of our former calculations on a number of collinear three-atom systems,<sup>8</sup> where the above values proved to be advantageous and safe. In the following, we illustrate the working of the algorithm on the development of the final RPs when starting from different initial curves. Eleven cases will be discussed and displayed by sets of distinct curves in Figures 1-6 showing the phases of the evolutions of curves. The sequences of approximating polygons in the fig-

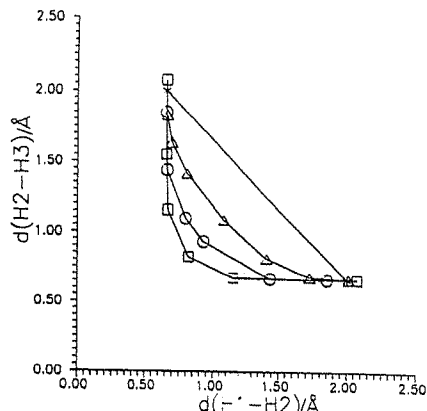


Figure 1. Evolution of an IRC section from a digon.

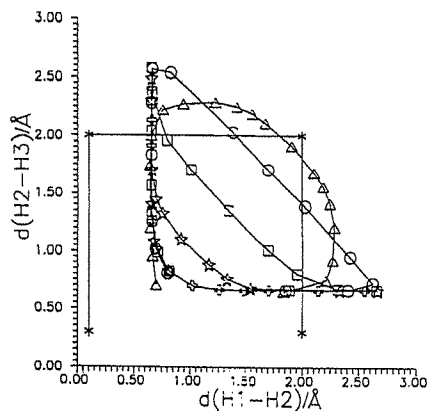


Figure 2. Evolution of an IRC section from a Π-shaped open polygon.

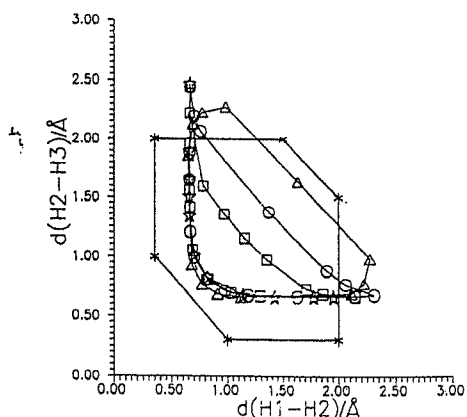


Figure 3. Evolution of an IRC section from a closed hexagon.

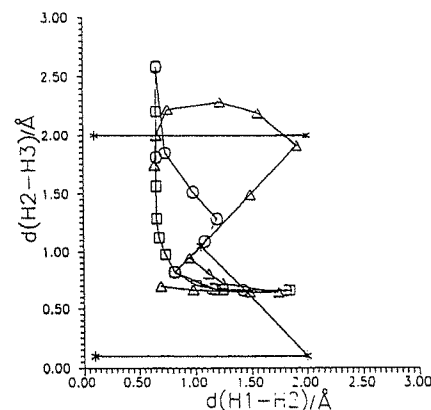


Figure 4. Evolution of an IRC section from an M-shaped open polygon.

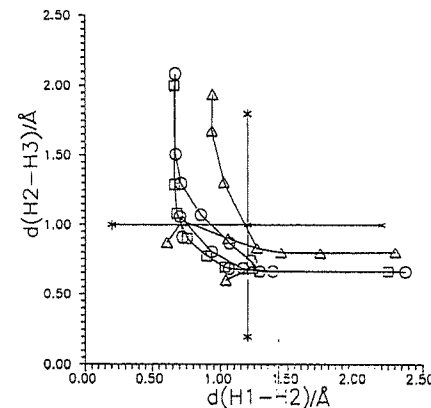


Figure 5. Evolution of an IRC section from a + shaped open polygon.

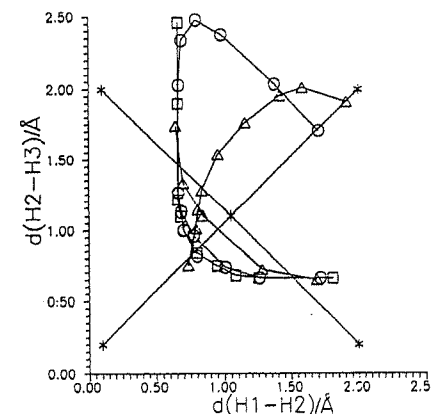


Figure 6. Evolution of an IRC section from an X-shaped open polygon.

ures will always be denoted in the following order: (first) \*, (second) Δ, (third) ○, (fourth) □, (fifth) ☆, and (sixth) ⚡.

Case 1

The initial curve was a section of a straight line (a digon) determined by the points (0.66, 2.00; 2.00, 0.66). Apart from the initial and final curves, two intermediate positions have also been shown in Figure 1.

Case 2

The initial curve was an L-shaped-right angle (an orthogon) determined by the points (0.30, 2.00; 0.30, 0.30; 2.00, 0.30). The next (second) curve shifted upward to the right while the vertex at (0.3, 0.3) disappeared and the curve lost its point. The third curve moved still further up and smoothed, and finally the last (fourth) curve showed the approximate IRC. Of course, if we used more points on the curves the final IRC would be nicely rounded (see Fig. 7).

Case 3

We started from a Greek capital letter Π-shaped open polygon given by the points (0.10, 0.30; 0.10, 2.00; 2.00, 2.00; 2.00, 0.30). From among all the investigated cases, this initial polygon was the least similar to the final IRC. This difference has been reflected in the highest computation time needed for the development of the final curve from the initial one (Table I). Six phases of the development are shown in Figure 2. Starting from the initial polygon, the evolution curves are going through the following main phases until reaching the final IRC. The top right section

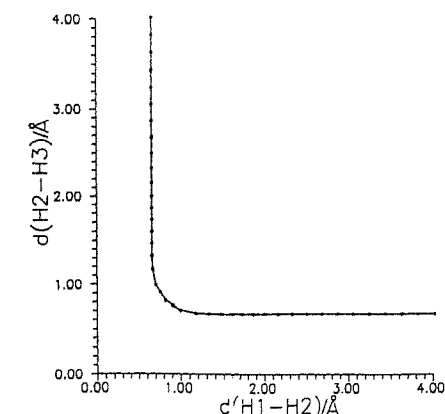


Figure 7. Complete IRC of the H<sub>2</sub> + H reaction as calculated by the DRRP-modified MNDO method.

\*For multidimensional cases, the convergence can be established by examining the Hausdorff distances between the successive trial polygons.<sup>5</sup>

**Table I.** Consecutive evolution curves indicated by \* (first), Δ (second), ○ (third), □ (fourth), ☆ (fifth), and ⬢ (sixth).

Figure	Number <i>N</i> of Iterations (s)					
	*	Δ	○	□	☆	⬢
1	0	7 (3877)	13 (5741)	39 (9899)		
2	0	4 (7234)	12 (17,245)	21 (30,576)	26 (38,281)	43 (49,488)
3	0	2 (6787)	6 (16,451)	9 (22,002)	25 (34,207)	
4	0	2 (7229)	13 (25,837)	19 (30,325)		
5	0	1 (3176)	4 (6307)	19 (14,708)		
6	0	2 (6224)	6 (13,945)	19 (29,319)		

first bulges outward, giving a concave curve, then it straightens and is becoming stepwise a deeper convex curve while the left leg of the Π-letter shifts parallel with itself, upward and to the right. Then, the bottom section of the left leg first bends inward, stepwise finding connection with the bottom section of the right leg bending also inward, and finally melting with the top section they give the approximate IRC curve (Fig. 2).

**Case 4**

The initial polygon (first curve) had the same shape as in case 3 except that it had been turned upside down and was determined by the points (0.66, 2.00; 0.66, 0.66; 2.00, 0.66; 2.00, 2.00). The starting position was much more advantageous than that in case 3; therefore, the computation time was much shorter. First, the left bottom vertex became more and more rounded while the vertical line from the right top bent toward left by going from concave to convex curve and finally adhering closely to the baseline formed lastly the approximate IRC.

**Case 5**

The initial curve was a closed tetragon (square) determined by the same points as in case 4. As the bottom left vertex moved inward and got rounded, the top right vertex first humped outward, then going through the stage of a straight line it became hollow, merging finally into the left bottom section to give the approximate IRC.

**Case 6**

Evolution of the IRC from a closed hexagon (vertices at 0.35, 2.00; 0.35, 1.00; 1.00, 0.30; 2.00, 0.30; 2.00, 1.50; 1.50, 2.00) can be seen (Fig. 3). This geometric form can be derived from a square whose diagonal two vertices at 0.35, 0.30; and 2.00, 2.00 have been cut off by two parallel straight lines. By this mutilation, the evolution of the final curve is accelerated compared to that of the original square. Disregarding this, in the course of evolution the shapes of the set of curves are similar to that of case 5 while the computation time was shorter.

**Case 7**

Starting from an open six-sided polygon (a heptagon with vertices at 0.55, 2.00; 0.55, 1.00; 1.00, 0.50; 2.00, 0.50; 2.00, 0.77; 1.00, 1.00; 1.00, 2.00), which was a rather advantageous situation for the searching procedure, the final curve in three stages developed in a short time (7923 s).

**Case 8**

The next initial curve was a block-letter capital T with vertices at 0.10, 2.00; 1.00, 2.00; 1.00, 0.10; 1.90, 2.00. After three phases of evolution of the IRC, a quasiconvergence could be reached in 16,192 s.

**Case 9**

The ninth trial polygon (an open pentagon) was a block-letter capital M lying prone with vertices at 0.10, 2.00; 2.00, 2.00; 1.05, 1.05; 2.00, 0.10; 0.10, 0.10. The evolution of the IRC in four stages is shown in Figure 4, the evolution time being 30,325 s.

**Cases 10 and 11**

The initial polygons were a standing and an oblique cross, respectively, determined by the points (0.2, 1.0; 1.2, 1.0; 2.2, 1.0; 1.2, 0.2; 1.2, 1.8) and (0.1, 2.0; 2.0, 0.2; 1.05, 1.1; 0.1, 0.2; 2.0, 2.0). The corresponding evolution curves in four phases are shown in Figures 5 and 6, respectively.

It is important to emphasize that in the present calculations illustrated by Figures 1–6 our aim was, naturally, not the determination of the complete RP but the demonstration of the high stability of the DDRP algorithm shown when starting from different initial curves/polygons. Therefore, we were satisfied by projecting the actual successive approximating polygons, obtained by relatively few iterations, to the RP and did not strive for determining as long a section of the RP as possible. If we wanted to calculate the whole RP (between rational limits, regarding that its ends extend to infinity), we would have to continue the iterations much further (a more complete RP of the H<sub>2</sub> + H reaction is displayed in Fig. 7). All our computations, of course, gave the same IRC, with an SP at 0.820 Å. The computation

times in seconds for the evolution phases in the *N*th iteration are summarized in Table I.

In the second part of our investigations, the shape and location of the initial curve were kept the same for all cases and the value of  $\epsilon$  at 0.3 was fixed while the values of the other two parameters,  $\eta$  (between 0.002 and 0.1) and  $\sigma$  (between 0.001 and 3.0), were varied. Starting from the chosen polygon (a concave tetragon with vertices at 0.50, 2.00; 0.50, 0.50; 2.00, 0.50; 1.00, 1.00) is advantageous to accelerate convergence and in this case the end of the procedure can easily be checked by observing the fusion of the sides of the tetragon into a solid line. For each pair of values of the varied parameters  $\eta$  and  $\sigma$ , the new evolution curve was output in every step. In each case, altogether 20 curves (including the initial one) were computed and recorded. The time  $T_{conv}$  needed to reach convergence was generally less than the total computation time  $T_{tot}$  necessary to determine all 20 curves. The data reflecting the variations of parameters  $\eta$  and  $\sigma$  and the related computation times are displayed in Table II. It is obvious from these data how important the right choice of parameters is. By enhancing the value of  $\eta$  at fixed values of  $\sigma$ , the total computation time will be higher and the differences in the computation times belonging to the smallest and largest values of  $\eta$  will even be drastic. Similarly, at fixed values of  $\sigma$  one can always find an optimal  $\eta$  value by which the computation time needed to reach convergence is the shortest. Further enhancement of  $\eta$  will increase also the value of  $T_{conv}$ . Then, the value of  $\eta$  was fixed while enhancing the value of  $\sigma$  from 0.001 to 3.0. The total computation time first reduced rapidly; then, from around  $\sigma = 0.1$  the gain in time became negligible. In this case, the change in  $T_{conv}$  was the same as that of  $T_{tot}$ , i.e., it reduced to the end. It is not a surprising although inconvenient experience of ours and still

useful information for users that the simultaneous enhancement of  $\eta$  and  $\sigma$  beyond a certain limit may cause numerical problems. This happened in an investigated case when  $\sigma \geq 0.3$  and  $\eta \geq 0.05$ . In this range for  $\sigma = 0.3$  and  $\eta \geq 0.05$ , the shapes of curves became diffuse. For  $\sigma = 1.0$  or 3.0 and  $\eta = 0.05$  or 0.1, the procedure became unstable, the points of the curve did not converge to the RP but deviated from it irregularly, the number of points grew rapidly, and finally, after exceeding the allowed dimension (presently 200) the program exited. It is important to emphasize that this kind of instability is not the usual property of the algorithm and normally does not occur but was due to the extremely bad parameter choice. The most advantageous ranges of parameter values were found to be in [0.01–0.1] for  $\sigma$  and in [0.005–0.05] for  $\eta$ . Even the minimum computational times  $T_{conv}$  fell into these ranges. It seems that the values of  $\sigma$  and  $\eta$  should be chosen either equal or near equal to each other to reach convergence in the shortest possible times. The best parameter choice proved to be  $\sigma = 0.1$  and  $\eta = 0.05$  (see Table II). Worth mentioning is that it is generally not practical to have the shortest computation time because in this case other problems may occur, e.g., for  $\sigma = 0.3$  and  $\eta = 0.05$  diffuse lines appeared.

Our results were also compared to those calculated by other methods. The searching procedure built in the MNDO program of the AMPAC 1.10 version gave an SP also at 0.820 Å, which agrees with ours. By the MNDO program (QCPE 353) and employing the above location of the SP taken from separate calculation, we determined and obtained the same RP as with the use of the DDRP method by starting from the points (4.0; 1.0) and (1.0; 4.0) using a steplength of 0.2 Å (Fig. 7). The only differences are in the numbers and locations of the points on the final IRC curves. Figures 8 and 9 show the

**Table II.** Effects of parameter variations on computing times.

$\sigma$	Time (s)	$\eta$				
		0.002	0.005	0.01	0.05	0.1
0.001	$T_{tot}$	16,214	24,581	37,416	142,208	246,012
	$T_{conv}$	16,214	13,371	13,258	19,449	23,733
0.003	$T_{tot}$	7294	9714	14,306	48,874	83,718
	$T_{conv}$	7294	4961	4754	6639	9769
0.01	$T_{tot}$	5024	5416	6036	17,095	28,416
	$T_{conv}$	5024	2298	1752	2191	3151
0.03	$T_{tot}$	4616	4853	4999	9310	15,626
	$T_{conv}$	4616	1734	1116	981	1491
0.1	$T_{tot}$	4585	4728	4954	8046 D	12,871 D
	$T_{conv}$	4585	1608	960	697 D	1056 D
0.3	$T_{tot}$	4585	4726	4908	17,265 D <sup>a</sup>	26,346 D <sup>a</sup>
	$T_{conv}$	4585	1606	931	670 D <sup>a</sup>	1224 D <sup>a</sup>
1.0	$T_{tot}$	4585	4726	4908	Dimension overflow	Dimension overflow
	$T_{conv}$	4585	1606	931		
3.0	$T_{tot}$	4586	4726	4908	Dimension overflow	Dimension overflow
	$T_{conv}$	4586	1607	931		

D, Diffuse lines, convergence cannot be determined definitely.  
<sup>a</sup>Number of points increases rapidly.

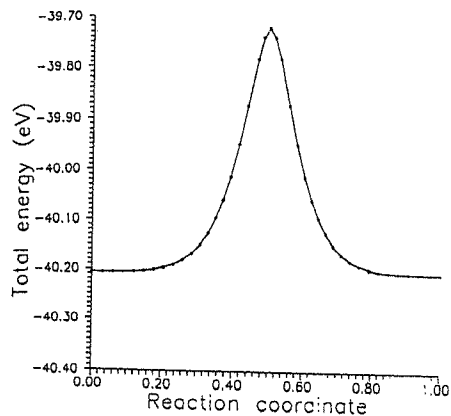


Figure 8. MNDO energies in the function of RC.

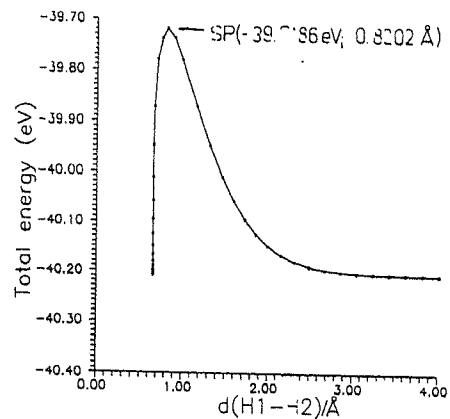


Figure 9. Curve energy vs. H1—H2 distance showing the location of the SP.

MNDO energies in the functions of the reaction coordinate (RC) and the H1—H2 distance, respectively, displaying the location of the SP.

The FORTRAN code for the algorithm used is to be distributed by QCPE.<sup>6</sup>

This work was supported by the Hungarian Scientific Research Fund (Grant OTKA: T4202).

## SUMMARY

We have shown that our DDRP algorithm generally behaves in a stable way. By starting from polygons of arbitrary geometric shapes,\* the IRC and SP of a simple collinear triatomic system can easily be computed. Our experiences on the  $H_2 + H$  reaction and other triatomic systems<sup>7,8</sup> raise hope that the method could be used with the same effectiveness on more complicated chemical reactions.<sup>15</sup> The run-time demand depends much on the choice of the initial polygon and the parameters, and in the present form of the program<sup>5,6</sup> it is higher than that of other searching procedures. However, because of the high parallelizability of our method drastic reduction in computation times can be expected in the near future after developing a program<sup>16</sup> to exploit this advantage and running it on a computer provided by parallel/vector facilities. This will hopefully make our method most useful for the theoretical investigations of fundamental reaction kinetic problems.

## References

1. L.L. Stachó and M.I. Bán, *Theor. Chim. Acta*, **83**, 433 (1992).
2. L.L. Stachó and M.I. Bán, *J. Math. Chem.*, **11**, 405 (1992).
3. L.L. Stachó and M.I. Bán, *Theor. Chim. Acta*, **84**, 535 (1993).
4. T. Poston and I. Stewart, *Catastrophe Theory and its Applications*, Pitman, London, 1978.
5. L.L. Stachó and M.I. Bán, *Comp. Chem.*, **17**, 21 (1993).
6. Gy. Dömötör, M.I. Bán, and L.L. Stachó, *QCPE*, accepted for distribution.
7. Gy. Dömötör, T. Körtvélyesi, and M.I. Bán, *Theor. Chim. Acta*, in preparation.
8. Gy. Dömötör, T. Körtvélyesi, M.I. Bán, T. Csendes, and L.L. Stachó, unpublished results.
9. K. Müller, *Angew. Chem.*, **92**, 1 (1980).
10. M.R. Peterson and I.G. Csizmadia, In *Molecular Structure and Conformation: Recent Advances, Progress in Theoretical Organic Chemistry*, vol. 3, I.G. Csizmadia, Ed., Elsevier, Amsterdam, 1982, p. 190.
11. E.G. Mezey, *Potential Energy Hypersurfaces*, Elsevier, Amsterdam, 1987.
12. D.A. Liotard, private communication.
13. D.A. Liotard, *Int. J. Quant. Chem.*, **43**, 723 (1992).
14. D.A. Liotard and J.-P. Penot, In *Numerical Methods in the Study of Critical Phenomena*, J. Della Dora, J. Demongeot, and B. Lacolle, Eds., Springer, Berlin, 1981, p. 213.
15. Gy. Dömötör, T. Körtvélyesi, and M.I. Bán, *Theor. Chim. Acta*, to appear.
16. Gy. Dömötör and M.I. Bán, in preparation.

\*The polygon can be either open or closed, can have any number of vertices, and can be situated almost anywhere in the space. Nevertheless, regardless of where we start searching from, finally we shall by all means find the SP, the only difference being in computation time and the only danger would be to get into other basins of extremal points or catchment regions.